

FSI Analysis of the Human Trachea under Impedance-Based Boundary Conditions

M. Malvè^{1,2}, A. Pérez del Palomar^{1,2}, S. Chandra³, E. Finol³, and M. Doblaré^{1,2}

¹ Group of Structural Mechanics and Materials Modeling, Aragón Institute of Engineering Research (I3A), University of Zaragoza, Spain

² Centro de Investigación Biomédica en Red en Bioingeniería, Biomateriales y Nanomedicina (CIBER-BBN), Zaragoza, Spain

³ Institute for Complex Engineered Systems (ICES), Carnegie Mellon University, 5000 Forbes Avenue, Pittsburg, USA

Abstract—This work is focused on the analysis of a healthy and a stenotic human trachea with aim to study flow patterns, wall stresses and deformations under physiological and pathological conditions. The two analyzed tracheal geometries, which include the first bifurcation after the carina, were obtained from computed tomography (CT) images of a healthy and a diseased patient respectively. Numerical simulations were performed through a finite element-based commercial software package, using a fluid-solid interaction (FSI) approach. Tracheal wall was modeled as a fiber reinforced hyperelastic material in which we modeled the anisotropy due to the orientation of the fibers. Impedance-based pressure waveforms were computed using a method originally developed for the cardiovascular system, where the resistance of the respiratory system was calculated taking into account the entire bronchial tree, modeled as binary fractal network. Performed simulations show the possibility of analyzing flow and wall behavior for healthy and pathological tracheas, being a useful tool capable to evaluate quantities that cannot be assessed *in vivo*, like shear and wall stresses, pressure drop and flow patterns and to derive parameters which in the future could help clinical decisions and improve surgical outcomes.

Keywords— Fluid Structure Interaction, impedance method, fiber reinforced material, bifurcation.

I. INTRODUCTION

The main components that constitute the trachea are the cartilaginous rings, and the muscular membrane that runs longitudinally and posteriorly to the trachea. Cartilaginous structures maintain the windpipe open despite the interthoracic pressure during the respiration. Smooth muscle contraction and transmural pressure generate bending and tensile stresses in the cartilage and collapse it to regulate the air flow and modulate the diameter of the airway [1]. Although a better understanding of how this process is performed and how the implantation of a prostheses affects the response of the trachea is not only important but challenging, few studies have analyzed the behavior of the trachea under physiological conditions. Understanding of the normal or forced breathing process in healthy and diseased trachea, distribution of pressure, shear and wall stresses in the airway wall, are important for clinical applications as for instance in order to design more convenient prostheses or for mechanical ventilation techniques.

Most of the developed numerical studies in the respiratory system till now analyzed the airflow pattern using rigid walls and approximated airways geometries [2,3]. Only few studies are based on an accurate airway geometry coming from computed tomography (CT) or magnetic resonance (MRI) [4,5,6]. The work developed by [7] is the first analyzing the behavior of the trachea using a FSI analysis but using simplified constitutive models of the trachea. More recently, [8] study the flow characteristics and stress distributions in the airways during inhalation. Through a FSI approach, they compared tracheal behavior using an isotropic and an orthotropic material model.

Regarding the constitutive behavior of the tracheal walls, only few studies have analyzed their mechanical behavior for humans [9,10].

The final aim of this work is to contribute to a better understanding of the response of the human trachea during natural breathing and forced ventilation. Moreover, we show a new possible way to solve the challenging aspect of imposing physiological boundary conditions by modeling the resistance of the entire respiratory system through the impedance computation.

II. MATERIALS AND METHODS

A. Solid model of the trachea

The finite element models of the human healthy and diseased trachea were made based on a CT performed to a 70 and a 56 years old patient. To identify the tracheal tissues, the cartilage rings could be isolated through their higher density.

With help of MIMICS[®], the different material densities could be distinguished through different tones of the gray scale. A full hexahedral mesh of around 40000 elements was made using ABAQUS Inc. for both geometries (see Fig. 1). To determine the properties of the different tissues of the trachea, different experimental tests were conducted. A complete description of these tests can be found in our previous works [11,12]. The histology revealed that in the cartilage rings, the collagen fibres run randomly, therefore

an isotropic material can be used to define its behaviour. However, the muscular membrane presented two perpendicular families of collagen fibres, one of the families run longitudinally and the other transversely. For cartilage, since there is no preferential orientation, a Neo-Hookean model, with strain energy density function (SEDF) defined as

$$\Psi = C_1(I_1 - 3)$$

was used to fit the experimental results. Concerning the smooth muscle, the well known Holzapfel strain energy function [13] for one family of fibres was used,

$$\Psi = C_1(I_1 - 3) + \frac{K_1}{2K_2} [\exp[K_2(I_4 - 1)^2] - 1] + \frac{K_3}{2K_4} [\exp[K_4(I_6 - 1)^2] - 1] + \frac{1}{D}(J - 1)^2$$

where C_1 is the material constant related to the ground substance, $K_i > 0$ are the parameters which identify the exponential behavior due to the presence of collagen fibers and D weights tissue incompressibility modulus [13].

B. Fluid model of the trachea

The fluid was assumed as Newtonian ($\rho = 1.225 \text{ Kg/m}^3$, $\mu = 1.83 \cdot 10^{-5} \text{ Kg/m s}$) and incompressible under unsteady flow conditions. Flow was assumed turbulent for the analyzed cases since the Reynolds numbers, based on the median tracheal section, at peak velocity, were in turbulent regime ($\text{Re}_{\text{healthy}} = 30000$, $\text{Re}_{\text{stenosis}} = 10000$). Finally, to model the air flow, the $K-\omega$ Model was used. Using the commercial software FEMAP[®] an unstructured tetrahedral grid of about 200000 elements was created.

C. Impedance-based boundary conditions

In this study we follow the approach used for the cardiovascular system by Olufsen et al. [14]. Starting from patient-specific spirometries performed by the two patients, we modeled the entire respiratory system as a fractal network in which we computed the impedance-based pressure waveforms.

The airways network resulted in a series of bifurcations composed by a series of parent and daughter bronchi, as shown in Figure 2 (a). Each parent bronchus bifurcates in two daughter bronchi following a scaling guided by the asymmetry factors α and β of the root parent r_{root} , according to equations:

$$r_{ij} = \alpha^i \beta^{j-i} r_{\text{root}}, 0 \leq i \leq j$$

$$(r_0)_{d1} = \alpha(r_0)_{pa}, (r_0)_{d2} = \beta(r_0)_{pa}$$

The structured tree continues branching until the radius of any bronchial segment is less than given minimum values r_{min} , as the alveolar radius ($\sim 10 \mu\text{m}$) where we assumed zero

impedance. Other relevant parameters describing the binary tree are the power exponent ξ , the asymmetry index γ and the area ratio η described by the equations:

$$\eta = \frac{(r_0)_{d1}^2 + (r_0)_{d2}^2}{(r_0)_{pa}^2}, \gamma = \frac{(r_0)_{d2}^2}{(r_0)_{d1}^2}$$

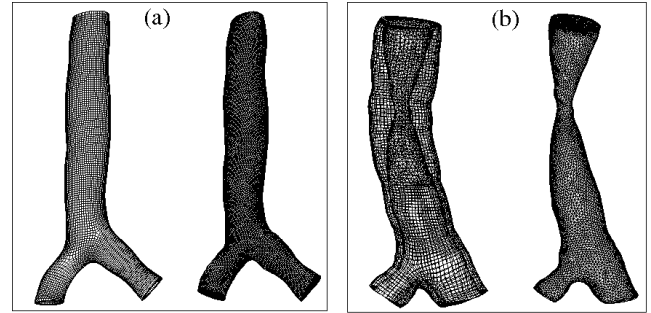


Fig. 1 Healthy (a) and stenotic (b) tracheal grids

From these equations, using $\xi = 2.33$, which is a good choice for a turbulent flow [14], and imposing $\gamma = 0.7$ following the studies of [15,16,17] on the human and rodent airways morphometry, $\eta = 1.1$. Using these parameters, the scaling factors α and β can be evaluated with the equations:

$$\alpha = (1 + \gamma^{\xi/2})^{-1/\xi}, \beta = \alpha \sqrt{\gamma}$$

Finally, the length of a given branch L can be related to the radius r_0 of each branch segment through the parameter $l_{\text{tr}} = L / r_0$. For this study we fixed an average value of $l_{\text{tr}} = 6$ [16,17].

Table 1 Parameters of the fractal network.

Radius	α	β	ξ	γ	η
$200 \leq r \leq 50$	0.8	0.67	2.33	0.7	1.1

In the Table 1, all the geometrical parameters used in the computations are given. Following the approach developed by Olufsen [14], the input impedance was evaluated at the beginning of each airway daughter as a function of the impedance at the end of the airway daughter

$$Z(0, \omega) = \frac{ig^{-1} \sin(\omega L / c) + Z(L, \omega) \cos(\omega L / c)}{\cos(\omega L / c) + igZ(L, \omega) \sin(\omega L / c)}$$

where L is the bronchial length, c is the wave-propagation velocity and $g = \sqrt{CA_0 K / \rho}$, with ρ air density, C wall

compliance, A_0 bronchial cross sectional area and $K = (1 - F_j)$. Finally $F_j = 2J_1(w_0)/w_0J_0(w_0)$ with J_0 and J_1

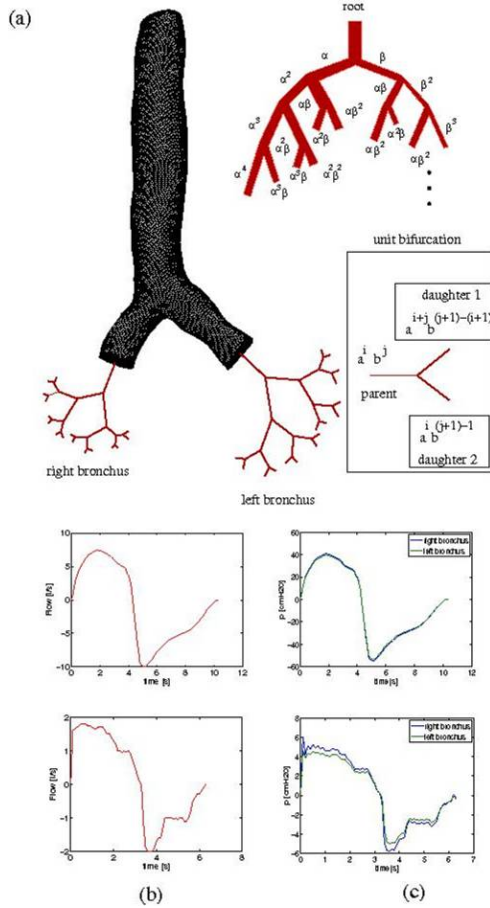


Fig. 2 Fractal networks (top) and flow and computed pressure waveforms (bottom)

zeroth and first Bessel function with $w=i^3w$ and $w=pr_0\omega/\mu$, i complex unity, μ air viscosity and w Womersley number.

The details of the recursive impedance calculation are given elsewhere [14]. In Figure 2, the spirometry (b) with the corresponding left and right bronchus pressure waveforms (c) used in the computations is sketched.

III. RESULTS AND DISCUSSION

A. Tracheal stresses and muscle deflections

The muscular deflection generates tensile stresses in the cartilage and modulates the airway diameter as reported also in [10]. Comparing the deformation of the cartilage rings between healthy and stenotic tracheas, it can be seen that

these open only partially respect to the healthy trachea. At inspiration the muscular membrane is in tension and the maximum value of the stress is 3 KPa. Showing only the tracheal cartilaginous parts as in the Figure 3 (b), it can be seen how they open during inspiration while the muscle expands, but in this case the registered deflections are smaller than those registered in the healthy trachea, due to the presence of the stenotic fibrous cap, which absorbs most of the load and restrains the cartilage opening capacity.

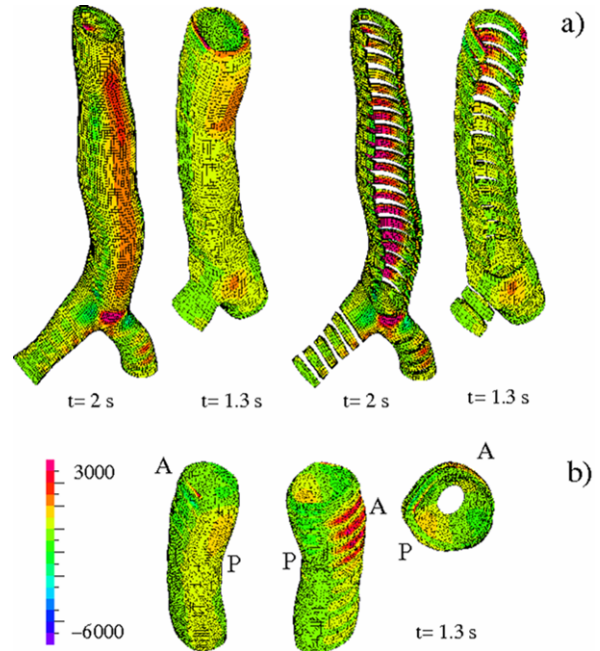


Fig. 3 Comparison of the maximum principal stresses (in [Pa]) of the complete model and of the cartilage rings (a) between healthy and stenotic trachea at peak flow during inspiration. In (b) the stresses distribution of the stenotic region is shown (P=posterior wall, A=anterior wall)

B. Comparison with CFD results

The relevance of the FSI results can be demonstrated through a comparison with a rigid wall model with the same geometries, in which we applied the same boundary conditions. Results showed differences in flow patterns for the healthy trachea, as well as differences of intra-tracheal pressure. For the stenotic trachea, at the constriction is visible a strong difference in the longitudinal vortex dimension between FSI and CFD computation (Fig 4 (a)). The values found are in the same range of other studies [18].

Moreover, discrepancies are also visible for the healthy trachea. The main difference is represented by the pressure

distribution (see Fig. 4 (b)). Stenotic tracheas show completely different pressure drop at the constriction while the pressure computed with FSI approach is two times that computed with CFD. We can conclude that FSI simulations are not only important for the computation of tensile stresses and strains but also in order to evaluate pressure drop. Moreover, tracheal wall deflections are not negligible and massive affect intra-tracheal flow patterns.

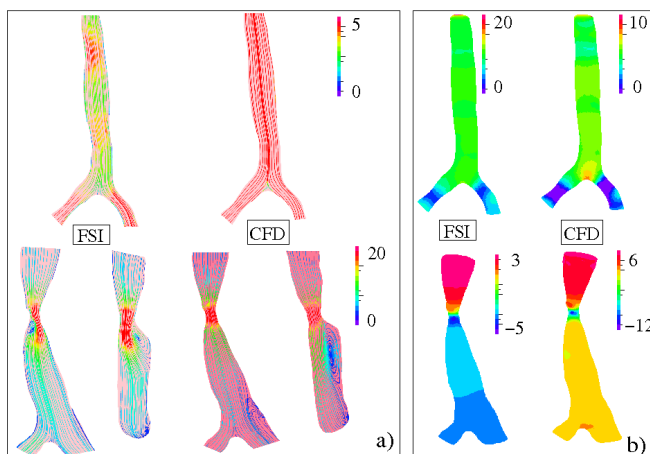


Fig. 4 Streamlines (a) and pressure distributions (b) in the healthy and stenotic trachea

IV. CONCLUSIONS

FSI unsteady airflow on a healthy and a stenotic trachea was carried out under impedance-based boundary conditions and turbulence modeling. We took into account the resistance of the respiratory system through the use of impedance-based method obtaining physiological flow features which qualitative agree with previous studies.

The importance of this work can be seen in the quantification of flow patterns and wall stresses inside different airway geometries such as those with stenotic and stented tracheas which numerical analysis could help surgical technique. In this way it could be possible to extract physical variables not assessable *in vivo*, as WSS, local pressure drops, muscular deflections and stresses.

ACKNOWLEDGMENT

This study was supported by the CIBER-BBN, an initiative funded by the VI National R&D&i Plan 2008-2011, Iniciativa Ingenio 2010, Consolider Program, CIBER Actions and financed by the Instituto de Salud Carlos III with assistance from the European Regional Development Fund

and by the research project PI07/90023. The authors wish to thank Christine M. Scotti (W.L. Gore & Associates, Inc. Flagstaff,AZ, USA).

REFERENCES

1. Lyubimov GA, (2001) The Physiological Function of the Posterior Tracheal Wall. Doklady Biological Science, 380: 421-423.
2. Ma and Lutchen (2006) An anatomically based hybrid computational model of the human lung and its application to low frequency oscillatory mechanics. Annals of Biom. Eng., 34(11): 1691-1704.
3. Nowak N, Kakade PP, Annapragada AV, (2003) Computational Fluid Dynamics simulation of airflow and aerosol deposition in the human lungs. Annals of Biom Eng, 57: 374-390.
4. Luo HY, Liu Y (2008) Modeling the bifurcating flow in a CT-scanned human lung airway, J of Biomech, 41: 2681-2688.
5. Liu Y, So RMC, Zhang CH (2002) Modeling the bifurcation flow in a human lung airway, 35: 465-473.
6. Liu Y, So RMC, Zhang CH (2003) Modeling the bifurcation flow in an asymmetric human lung airway, J of Biomech, 36: 951-959.
7. Wall WA, Rabczuk T, Fluid-structure Interaction in lower airways of CT-based lung geometries (2008) Internat. J. for Num. Meth. In Fluids, 57: 653-675.
8. Koombua K, Pidaparti RM (2008) Inhalation Induced Stresses and Flow Characteristics in Human Airways through Fluid-Structure Interaction Analysis. Modeling and Simulation in Eng., 2008:1-9.
9. Rains JK, Bert JL, Roberts CR, Paré PD (1992) Mechanical Properties of human tracheal cartilage, J of Biomech, 72: 219-225.
10. Roberts CR, Rains JK, Paré PD, Walker DC, Wiggs B, Bert JL, (1998) Ultrastructure and tensile properties of tracheal cartilage, J of Biomech, 31: 81-86.
11. Trabelsi O, Pérez del Palomar A, López-Villalobos JL, Ginel A, Doblare M, (2010) Experimental characterization and constitutive modeling of the mechanical behavior of the human trachea, Med Eng and Physics, 32: 76-82.
12. Malvè M, Pérez el Palomar A, López-Villalobos JL, Ginel A, Doblare M, (2010) FSI analysis of the coughing mechanism in a human trachea, Annals of Biomed Eng., 38: 1556-1565.
13. Holzapfel GA, Nonlinear Solid Mechanics. Wiley, New York, 2000.
14. Olufsen MS, (1999) A structured tree outflow condition for blood flow in larger systemic arteries, American J of Phys, 276: H257-H268.
15. Latourelle JC, Gillis HL, Lutchen R (2001) Exact morphometric modeling of rat lungs for predicting mechanical impedance, Resp. Phys. And Neurob., 127:75-85.
16. Horsfield K., Woldenberg ML (1989), Diameter of cross sectional areas of branches in the human pulmonary arterial tree, Anat. Rec., 223:245-351.
17. Horsfield K, Dart G, Olson DE, Filley GF, Cumming G, (1971) Model of the human bronchial tree, J Appl Physiol, 31:207-217.
18. Brouns M, Jayaraju ST, Lacor C, De MEy J, Noppen M, Vincken W, Verbanck S (2006) J Appl Physiol, 102:1178-1184.

Author: Mauro Malvè
 Institute: GEMM Group I3A, University of Zaragoza
 Street: Calle María de Luna s/n, 50018
 City: Zaragoza
 Country: Spain
 Email: mmalve@unizar.es